Plant Science 253 (2016) 31–39

Contents lists available at ScienceDirect

Plant Science

journal homepage: www.elsevier.com/locate/plantsci

Knocking down expression of the auxin-amidohydrolase *IAR3* alters defense responses in Solanaceae family plants

Sebastian D'Ippolito[a], Radomira Vankova[b], Matthieu H.A.J. Joosten[c,d], Claudia A. Casalongué[a,*], Diego F. Fiol[a,*]

[a] *Instituto de Investigaciones Biológicas IIB-Consejo Nacional de Investigaciones, Científicas y Técnicas, Universidad Nacional de Mar del Plata, Mar del Plata, Argentina*
[b] *Institute of Experimental Botany, Academy of Sciences of the Czech Republic, Prague, Czech Republic*
[c] *Laboratory of Phytopathology, Wageningen University, Wageningen, The Netherlands*
[d] *Centre for BioSystems Genomics, Wageningen, The Netherlands*

ARTICLE INFO

Article history:
Received 2 June 2016
Received in revised form
12 September 2016
Accepted 20 September 2016
Available online 21 September 2016

Keywords:
Auxin
Biotic stress
Cladosporium fulvum
Indole-3-acetic acid amido hydrolases
Nicotiana benthamiana
Phytophthora infestans
Solanum lycopersicum

ABSTRACT

In plants, indole-3-acetic acid (IAA) amido hydrolases (AHs) participate in auxin homeostasis by releasing free IAA from IAA-amino acid conjugates. We investigated the role of IAR3, a member of the IAA amido hydrolase family, in the response of Solanaceous plants challenged by biotrophic and hemibiotrophic pathogens. By means of genome inspection and phylogenic analysis we firstly identified IAA-AH sequences and putative IAR3 orthologs in *Nicotiana benthamiana*, tomato and potato. We evaluated the involvement of *IAR3* genes in defense responses by using virus-induced gene silencing. We observed that *N. benthamiana* and tomato plants with knocked-down expression of *IAR3* genes contained lower levels of free IAA and presented altered responses to pathogen attack, including enhanced basal defenses and higher tolerance to infection in susceptible plants. We showed that *IAR3* genes are consistently up-regulated in *N. benthamiana* and tomato upon inoculation with *Phytophthora infestans* and *Cladosporium fulvum* respectively. However, *IAR3* expression decreased significantly when hypersensitive response was triggered in transgenic tomato plants coexpressing the *Cf-4* resistance gene and the avirulence factor *Avr4*. Altogether, our results indicate that changes in *IAR3* expression lead to alteration in auxin homeostasis that ultimately affects plant defense responses.

1. Introduction

The plant hormone indole-3-acetic acid (IAA) is the most common natural auxin. IAA plays essential roles throughout the plant life cycle participating in growth, development and responses against environmental stresses. Plants coordinate IAA homeostasis by regulating its biosynthesis, transport, oxidation, degradation and conjugation [1,2]. Auxin conjugates play important roles as storage forms for the active IAA. Auxin conjugates can be divided in low molecular weight conjugates (with sugars or aminoacid moieties, either via ester or amide bonds respectively) and high molecular weight conjugates, with peptides and proteins via amide bond. In particular, the formation of IAA-amido-conjugates through the conjugation of IAA with amino acids results in the hormone inactivation and also creates a reservoir of IAA that can be rapidly made available by IAA amido-hydrolase (IAA-AH) enzymes [3]. In Arabidopsis, seven genes encoding IAA-AHs have been identified [4]. Gene sequences for IAA-AHs have been also identified in other plant species, including *Triticum aestivum*, *Brassica rapa* and *Medicago truncatula* [5–7]. However, the role of the amido-hydrolase enzymes in the physiology of the plant has not been well determined yet. IAA amido-hydrolases could be promiscuous enzymes and their respective conjugated IAA substrates could have additional functions associated with plant defense mechanisms [7].

The ability of many plant pathogenic microorganisms to produce IAA during infection also points to the involvement of this hormone in plant disease development [8,9]. In particular, disruption of IAA-conjugate metabolism, leading to IAA-Asp accumulation, has been reported as part of a strategy to promote disease by the necrotroph *Botrytis cinerea* and the hemibiotroph *Pseudomonas syringae* infecting Arabidopsis *thaliana* [10]. Previously, we identified a potato transcript coding for a protein that is 67%

* Corresponding authors.
E-mail addresses: dippolit@mdp.edu.ar (S. D'Ippolito), vankova@ueb.cas.cz (R. Vankova), matthieu.joosten@wur.nl (M.H.A.J. Joosten), casalong@mdp.edu.ar (C.A. Casalongué), diefiol@mdp.edu.ar (D.F. Fiol).

http://dx.doi.org/10.1016/j.plantsci.2016.09.008
0168-9452/

identical to *At*IAR3 which was also up-regulated in potato tubers upon infection with *Fusarium solani* f. sp. *eumartii* [11].

In this work, we studied the involvement of *IAR3* gene in defense response in two plant-pathogen interactions; *Nicotiana benthamiana* inoculated with an avirulent strain of *Phytophthora infestans* (an incompatible interaction) and tomato (*Solanum lycopersicum*) inoculated with a virulent strain of *Cladosporium fulvum* (a compatible model). By means of virus induced gene silencing experiments and gene expression analysis we conclude that modifications in *IAR3* genes expression promote changes in auxin homeostasis that affect pathogen proliferation in plant tissues.

2. Material and methods

2.1. Plant material and growth conditions

Nicotiana benthamiana, Solanum lycopersicum "Money Maker"-Cf4 (MM-Cf4) and "Money Maker"-Cf0 (MM-Cf0) plants were grown on organic substrate and vermiculite (8:1) and placed in the greenhouse with the following settings: 25 °C with 60% relative humidity under 120 μmol photons/m^2 s^{-1} with 16:8 h light:dark cycles.

Tomato plants offspring expressing the resistance *Cf-4* (=*Hcr9-4D*) gene and the avirulence gene *Avr4* from *Cladosporium fulvum* were generated by crossing transgenic MM-Cf0 plants expressing *Avr4* ("Money Maker"-*Cf0*:*Avr4*) to transgenic "Money Maker"-Cf0:*Hcr9-4D* ("Money Maker"-Cf4) plants as described earlier [12,13]. Seeds of the obtained *Cf-4*/*Avr4* and parental lines were germinated and kept for 7 days under normal daylight conditions at room temperature as described by [14]. At day 8 after germination seedlings were incubated at 33 °C and 100% relative humidity (RH) under a 16:8 h light:dark regime for an additional 14 days. In order to promote the initiation of the response induced by Cf-4/Avr4 interaction, seedlings were shifted to 20 °C/70% RH [15].

2.2. Generation of microbial inoculums

Phytophthora infestans (Mont.) de Bary (race R2 R3 R6 R7 R9, mating type A2) was isolated from infected leaflets of potato and routinely grown on potato slices for one week at 18 °C and 90% RH in the dark [16]. Sporulation was induced by incubation of mycelium over night in water at 4 °C. Sporangiospores were isolated by filtration through a 10-μm nylon mesh. Spores were counted under an optic microscope (Nikon Eclipse E200) by using a Neubauer chamber and inoculations were performed with a suspension of 2×10^4 spores/ml. *C. fulvum* race 5, that express *Avr4* and contains a *pGPD:GUS* transgene expressing the *GUS* gene under control of the constitutive glyceraldehyde-3-P dehydrogenase promoter (pGPD) was cultured on potato dextrose agar at room temperature in the dark. After 10 days, spores were isolated and tomato plants were inoculated at the lower side of the leaves, as described by [17].

2.3. Silencing of N. benthamiana and tomato plants

Construction of silencing vectors was performed as described (Liu et al., 2002a; Liu *et al.*, 2002b). Tobacco rattle virus (TRV)-based binary vectors pTRV1 and pTRV2 were obtained from Dr. S. P. Dinesh-Kumar (UC Davis, USA). For pTRV2:*IAR31* construction, a 339 bp fragment corresponding to *Solanum tuberosum IAR31* from position 316 to 654 with respect to the ATG initiation codon (see table S1 for primer sequences) was subcloned, digested with *BamHI*/*XhoI* and ligated into *BamHI*/*XhoI*-digested pTRV2. The resulting pTRV2:*IAR31* silencing vector was transformed to *Agrobacterium tumefaciens* strain GV3101 by electroporation [18]. A non-functional 396 bp fragment of the β-*glucuronidase* gene (*GUS*) of *E. coli*, with no significant homology with any gene in Solanaceous plants, was cloned into pTRV2 (pTRV2:*GUS*) and used as a control [19]. Constructions pTRV:*Cf-4* and pTRV:*PDS* have been previously described [20,21]. pTRV2:*PDS* was used as a control in VIGS assays; *phytoene desaturase* (*PDS*) silencing caused by pTRV2:PDS leads to the inhibition of carotenoid synthesis and a photo-bleached phenotype [22]. Equal aliquots of *A. tumefaciens* containing pTRV1 and pTRV2:*GUS*, pTRV2:*IAR31*, pTRV2:*PDS* or pTRV2:*Cf-4* were mixed to OD_{600} = 1.0 and used to infiltrate the abaxial side of the leaves of 3-week-old *N. benthamiana* plants or alternatively, 10-day-old tomato seedlings. Five plants were infiltrated with the mixed cultures containing pTRV1 and either pTRV2:*IAR3*, pTRV2:*GUS* or pTRV2:*PDS* in each experiment. Targeting of *IAR3* in MM-Cf4 and MM-Cf0 tomato plants was performed similarly using the same pTRV constructs. Additionally, MM-Cf4 tomato plants were inoculated with pTRV:*Cf-4* as control.

2.4. P. infestans inoculations and growth quantification

Three-week-old *N. benthamiana* plants were inoculated with *P. infestans* by infiltration of 100 μl of a 10 mM $MgCl_2$ solution containing 2×10^4 spores/ml on the abaxial and right sides of detached leaves. Control plants were mock-inoculated with 100 μl of 10 mM $MgCl_2$ solution on the left side of the leaf. VIGS-silenced plants were inoculated 21 days after infiltration with the recombinant virus targeting the gene to be silenced. Detached leaves were placed in Petri dishes with 16:8 h light:dark cycles at 18 °C under 120 μmol photons/m^2 s^{-1}. Hypersensitive response (HR) development was scored daily. Leaf disks of 1.5 cm diameter were dissected from the area surrounding the inoculated site at 0, 24 and 72 h post inoculation (hpi) and used for determination of viable *P. infestans* or frozen in liquid nitrogen and stored at −80 °C for RNA or protein extraction.

Determination of viable pathogen on inoculated leaves was assessed by a growth assay in fresh media plates. Leaf disks dissected from the inoculated area were incubated on potato dextrose agar by 48 h in darkness at 18 °C. Mycelium growth was photographed and an index of the oomycete growth was calculated by using ImageJ software (National Institutes of Health; http://rsb.info.nih.gov/ij).

2.5. C. fulvum inoculations and GUS measurements in MM-Cf0 and MM-Cf4 tomato plants

C. fulvum conidial suspensions (OD_{600} = 0.6) were used to inoculate MM-Cf0 and MM-Cf4 tomato plants by spraying 3 weeks after inoculation *IAR3* silencing. Thirteen days later, 2 to 4 leaflets of putatively silenced leaves (as determined by the observation of bleached phenotype occurrence in PDS silencing experiments) from at least 5 plants were harvested and vacuum-infiltrated with X-gluc buffer (0.1 M NaPO4, pH 7.0, 1% Triton X-100, 1% DMSO, 10 mM EDTA and 1 mg/ mL X-gluc). Leaflets were incubated overnight at 37 °C in the darkness, distained with 70% ethanol and photographed. Blue staining was quantified using ImageJ software (National Institutes of Health; http://rsb.info.nih.gov/ij). Leaflets were harvested, immediately frozen in liquid nitrogen, and stored at −80 °C at the indicated times for RNA extraction.

2.6. Plant phenotypic analysis

Phenotypes of pTRV2:*IAR31*- and pTRV2:*GUS*-infiltrated *N. benthamiana* plants were analyzed 3 weeks post viral inoculation. Relative values of leaf area and plant height were calculated using ImageJ software (National Institutes of Health; http://rsb.info.nih.gov/ij).

2.7. RNA isolation, cDNA synthesis and PCR analysis

RNA was isolated from leaf disks dissected from the inoculated area using Trizol reagent (Invitrogen, USA) following the manufacturerís instructions. RNA (2 μg) was reverse-transcribed in the presence of oligo dT primers (Biodynamics SRL, Argentina) into cDNA using ImProm II first strand synthesis for RT-PCR kit (Promega, USA). Semi-quantitative PCR was performed using a MasterCycler (Eppendorf) under the following cycling parameters: 94 °C for 1 min, 30 cycles of 94 °C for 30 s, 60 °C for 30 s, 72 °C for 1 min and 72 °C for 5 min. Digitalized images of PCR products resolved in agarose gels were quantified using ImageJ software (National Institutes of Health; http://rsb.info.nih.gov/ij). Real Time quantitative PCR (qPCR) was performed using SYBR Green Master Mix (PE Applied Biosystems) in an ABI Step One 700 (PE Applied Biosystems). qPCR parameters were as follows: 95 °C for 10 min, followed by 40 cycles of 95 °C for 30 s, 60 °C for 30 s and 72 °C for 30 s. Results were normalized to actin content and expressed as fold-change over controls using the comparative cycle threshold (CT) method (ΔΔCT) [23]. PCR products were analyzed by melting curve analysis and agarose gel electrophoresis to confirm the presence of a single product. Gene-specific primer sequences were designed with Primer 3 software [24] and are listed in table S1.

2.8. Western blot assays

Total protein was extracted from pTRV2:*GUS*- or pTRV2:*IAR31*-infiltrated *N. benthamiana* leaf disks dissected from the area surrounding the inoculated spot at 2 days post inoculation (dpi) with *P. infestans*. Tissue was ground in 50 mM sodium acetate pH 5.2, 0.1% β mercaptoethanol, 0.5 M NaCl using a glass homogenizer. Proteins were separated on 12% SDS gels, blotted onto nitrocellulose membranes and analyzed by western blot using an anti-chitinase antibody (1:5000) obtained from Dr. E. Kombrink (Max-Planck-Institut für Züchtungsforschung, Cologne, Germany). Alkaline phosphatase conjugated goat anti rabbit secondary antibody (Sigma) and alkaline phosphatase staining kit (Sigma-Aldrich, USA) were used to develop the western blot. Digitalized images of revealed blots were used to quantify band intensity using ImageJ software (National Institutes of Health; http://rsb.info.nih.gov/ij). The blots were previously stained with Ponceau S to confirm equal protein loading.

2.9. IAA measurements

Plant hormones were purified and analyzed according to [25,26]. Leaves pooled from 5 to 7 plants were ground in liquid nitrogen and the powder was lyophilized. Samples for each condition (ca. 300 mg fresh weight) were homogenized and extracted with methanol/water/formic acid (15/4/1, v/v/v) and deuterium-labeled internal standards (10 pmol per sample) were added. The extract was cleaned using a SPE-C18 column (SepPak-C18, Waters) and compounds were fractionated using a reverse phase–cation exchange SPE column (Oasis-MCX, Waters). The fraction eluted with methanol contained IAA and derivatives. Auxins were separated by HPLC (Ultimate 3000, Dionex) and quantified using a hybrid triple quadrupole/linear ion trap mass spectrometer (3200 Q TRAP, Applied Biosystems).

3. Results

3.1. IAR3 homologs in S. tuberosum, S. lycopersicum and N. benthamiana

To identify *IAA-AH* gene sequences we inspected genomic databases of *S. tuberosum* (PGSC_DM_v3.4 Release), *S. lycopersicum* (ITAG2.3 Release) and the *N. benthamiana* draft genome (Niben.genome.v1.0.1 Release), using BLAST analysis with Arabidopsis sequences as queries. We found 8 *IAA-AHs* in *S. tuberosum*, 7 in *S. lycopersicum* and 12 in *N. benthamiana*. (Table S2). Translated nucleotide sequences were subjected to phylogenetic analysis, together with *A. thaliana IAA-AH* sequences corresponding to IAA-Leucine Resistant1 (ILR1) and ILR1-like (ILL) families (Fig. 1, Table S2). Solanaceae proteins were named according to their phylogenetic clustering and homology with *A. thaliana* proteins. Two IAR3 branches were identified. One branch, depicted in bold characters in Fig. 1, included StIAR31 (the protein coded by the previously identified potato transcript up-regulated upon biotic stress), SlIAR31, NbIAR31, NbIAR32 and Arabidopsis IAR3 and ILL5. The second branch contained StIAR32, SlIAR32, NbIAR33, NbIAR34; all of them Solanaceous sequences.

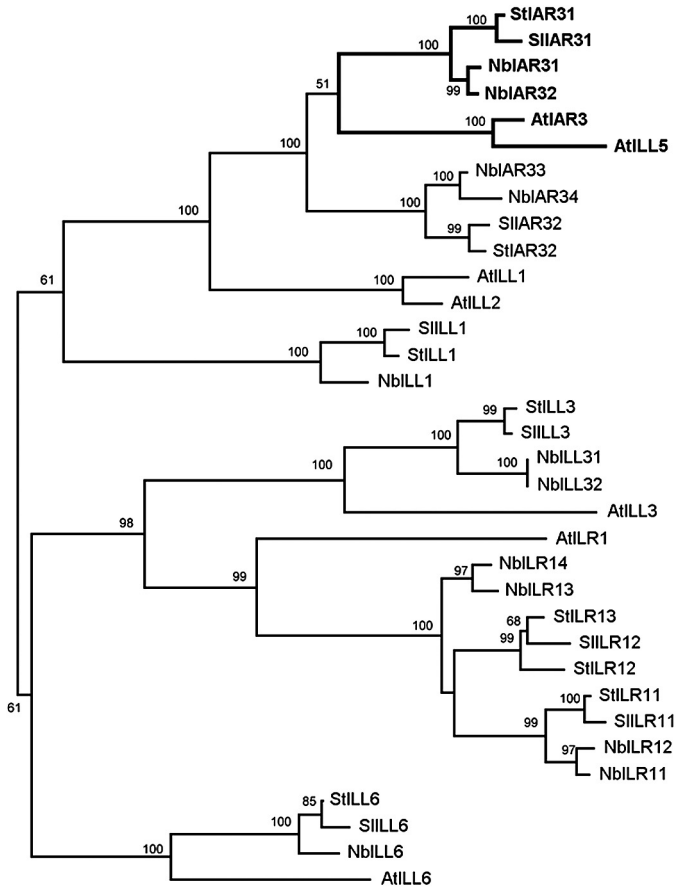

Fig. 1. Phylogenetic tree of 32 IAA-AH protein sequences from *A. thaliana*, *S. tuberosum*, *S. lycopersicum* and *N. benthamiana*. Details on the genes included in the phylogeny are listed in Table S2. Protein sequences were aligned with ClustalW and phylogenetic analysis was performed with MEGA5, using the Neighbor-Joining method [50]. Numbers next to the branches indicate the percentage of replicate trees in which the associated taxa will cluster together in the bootstrap test (1000 replicates).

3.2. IAR3 gene expression is up-regulated in P. infestans-inoculated N. benthamiana leaves

The expression of the newly identified *N. benthamiana IAR3* genes (*NbIAR31*, *NbIAR32*, *NbIAR33* and *NbIAR34*) was analyzed in plants inoculated with a *P. infestans* strain that generates an incompatible interaction. An incompatible interaction is characterized by the appearance of necrotic spots containing dead plant cells at the sites of pathogen inoculation, a plant response referred to as

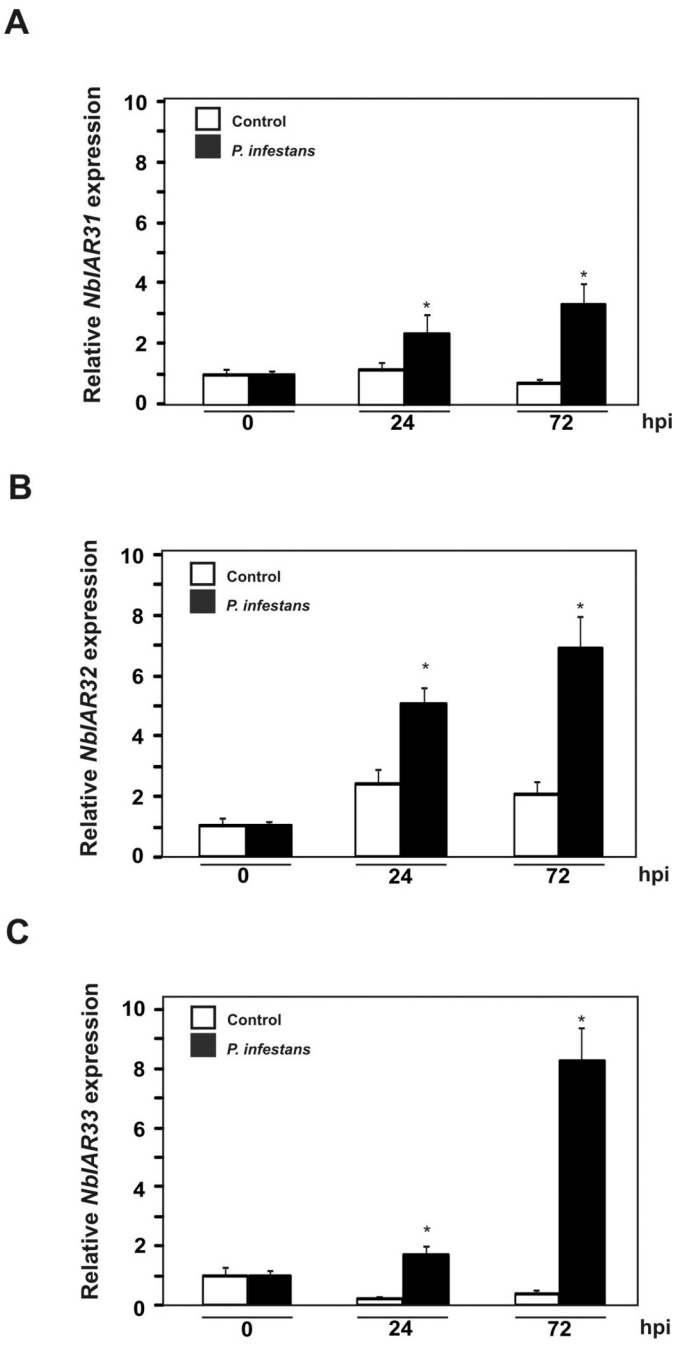

Fig. 2. Real Time qPCR analysis of *NbIAR31* (A), *NbIAR32* (B), *NbIAR33* and *NbIAR34* (C) expression in *P. infestans*-inoculated *N. benthamiana* plants. Expression levels are relative to time 0 in infected and control plants. Error bars represent the standard deviation from three biological replicates. Asterisks indicate significant differences as assessed by Student's *t*-test $P < 0.05$.

the hypersensitive response (HR). This type of programmed cell death requires recognition of the pathogen by the plant, followed by signal transduction and finally activation of several plant defense genes. To assess a putative role for *N. benthamiana IAR3* genes in this type of interaction, transcript levels of *NbIAR31*, *NbIAR32* and *NbIAR33* were measured in *P. infestans* inoculated and non-inoculated plants. The transcript levels corresponding to each of the 3 genes were higher in inoculated plants at 24 and 72 hpi, as compared with control plants (Fig. 2). On the other hand, expression of *NbIAR34* was undetectable under control conditions and remained unaltered upon the inoculation (data not shown). Occurrence of the

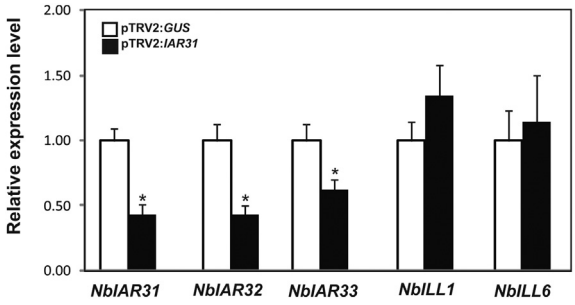

Fig. 3. Real Time qPCR analysis of *IAA-AH* gene expression in plants inoculated with recombinant pTRV constructs. *NbIAR31*, *NbIAR32*, *NbIAR33*, *NbIAR32*, *NbILL1* and *NbILL6* transcripts were quantified at 21 dpi in plants infiltrated with Agrobacterium carrying pTRV2:*GUS* or pTRV2:*IAR31*. Transcript levels are relative to values of pTRV2:*GUS*-infiltrated plants. Error bars represent the standard deviation from three biological replicates. Asterisks indicate significant differences as assessed by Student's *t*-test $P < 0.05$.

HR was confirmed by determining the transcript level of harpin-induced protein 1 (HIN1), a molecular marker for the occurrence of HR [27]. HIN1 was up-regulated at 24 h after *P. infestans* inoculation, indicating HR (Fig. S1).

3.3. *Knocking down of IAR3 results in a stunted* N. benthamiana *phenotype*

As a first approach to conduct VIGS in *N. benthamiana* plants, silencing of *PDS* gene was performed to set up experimental conditions and timing for assays. The *PDS* suppression was early visible as photobleaching at 14 dpi with the Agrobacterium strain carrying the pTRV2:*PDS* construct and it became clearer at 21 dpi, so this time point was chosen for the subsequent analysis (Fig. S2). *IAR3* transcript levels were analyzed in pTRV2:*IAR31*- and pTRV2:*GUS*-infiltrated plants. *NbIAR31*, *NbIAR32* and *NbIAR33* transcript levels were lower in pTRV2:*IAR31*-infiltrated plants, as compared to the pTRV2:*GUS*-infiltrated control plants (Fig. 3). *NbIAR31* and *NbIAR32* transcript levels were both 57% lower than the control, whereas *NbIAR33* transcript level was 37% lower than th were harvested, immediately frozen in liquid nitrogen, and stored e control. The stronger silencing of the *NbIAR31* and *NbIAR32* genes was according to our expectations, given the identity of these genes with the *StIAR31* fragment used in the silencing vector (92.3%, 92% and 74.0% identity in ungapped aligned regions to *NbIAR31*, *NbIAR32* and *NbIAR33* respectively) (Fig. S3). In contrast, transcript levels of the more distantly related IAA-AH family members, *NbILL1* and *NbILL6* did not change significantly in the pTRV2:*IAR31*-infiltrated plants respect to the pTRV2:*GUS*-infiltrated control plants (Fig. 3). Interestingly, pTRV2:*IAR31*-infiltrated plants consistently displayed a stunted phenotype, showing a decrease of 26% in height compared with control plants at 21 dpi (Fig. 4). In addition, a decrease of 33% in the total leaf area was also measured in pTRV2:*IAR31*-infiltrated plants (Fig. S4). Free IAA levels decreased in pTRV2:*IAR31*-infiltrated *N. benthamiana* plants. Free IAA and IAA derivatives were analyzed in pTRV2:*IAR31*- and pTRV2:*GUS*-infiltrated plants. The levels of free IAA decreased to about 40% in pTRV2:*IAR31*- as compared with pTRV2:*GUS*-infiltrated plants (Table 1). The levels of the inactive derivative oxo-IAA, which is the product of ring oxidation, decreased also to about 40% in the pTRV2:*IAR31*-infiltrated plants. On the other hand, the levels of the IAA-amino acid conjugates IAA-Asp and IAA-Glu, both considered to be inactive and not hydrolysable in Arabidopsis, showed no differences between the pTRV2:*GUS*- and pTRV2:*IAR31*-infiltrated plants. Other IAA-amino acid conjugates such as IAA-Ala and IAA-Leu could not be detected by the analytical method used.

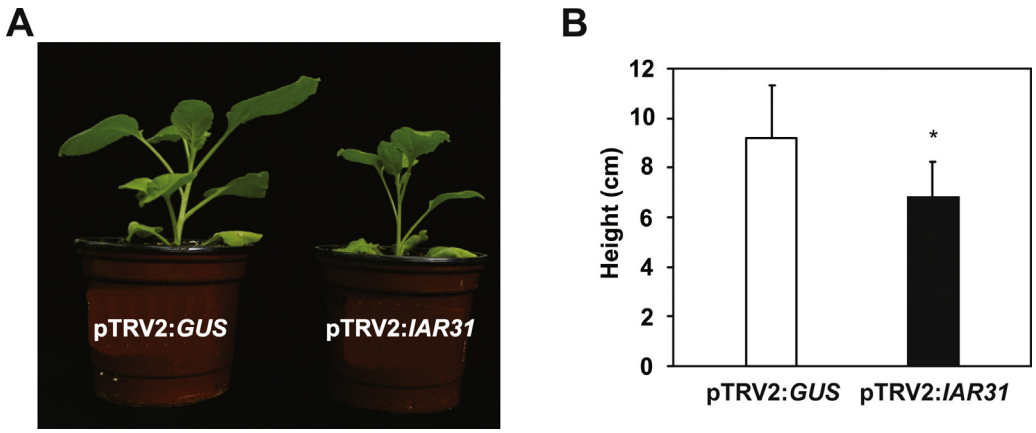

Fig. 4. Phenotype of pTRV2:*IAR31*-infiltrated N. benthamiana at 21 dpi (A) Plants infiltrated with pTRV2:*GUS* or pTRV2:*IAR31*. (B) Height of pTRV2:*IAR31*–infiltrated and pTRV2:*GUS*-infiltrated control plants. Values represent the average obtained for at least four independent experiments, in which at least five plants were included. Asterisk indicates significant difference as assessed by Student's *t*-test $P < 0.05$.

Table 1
Levels of free IAA and IAA derivatives in non-treated, pTRV2:*GUS*- and pTRV2:*IAR31*-infiltrated *N. benthamiana* plants. Levels are indicated in pmol/g FW. Different letters in the same column indicate significant differences as assessed by Student's *t* test $P < 0.05$.

	IAA	IAA-Asp	IAA-Glu	OxIAA
Non-treated	$439.39^{a} \pm 34.1$	$53.57^{a} \pm 5.4$	$19.17^{a} \pm 3.24$	$1451.70^{a} \pm 335.11$
pTRV2:*GUS*- infiltrated	$564.72^{b} \pm 38.57$	$86.19^{b} \pm 13.31$	$23.53^{a} \pm 2.42$	$2365.89^{b} \pm 183.96$
pTRV2:*IAR31*-infiltrated	$224.10^{c} \pm 38.02$	$91.37^{b} \pm 5.73$	$23.36^{a} \pm 3.85$	$925.28^{c} \pm 92.47$

3.4. *pTRV2:IAR31-infiltrated* N. benthamiana *plants showed an altered response to* P. infestans *inoculation*

Detached leaves from pTRV2:*IAR31*- and pTRV2:*GUS*-infiltrated *N. benthamiana* plants at 21 dpi, were inoculated with *P. infestans* or a $MgCl_2$ solution as a control. The progression of the plant response to the inoculation was monitored daily. Necrotic lesions resulting from the incompatible interaction were observed in both pTRV2:*GUS*- and pTRV2:*IAR31*-infiltrated leaves at 2 dpi. However, pTRV2:*IAR31*-infiltrated plants showed larger necrotic lesions than pTRV2:*GUS*-infiltrated plants (Fig. 5A), suggesting an alteration in the HR. In order to evaluate the responses displayed, *P. infestans* growth was quantified in leaf disks from pTRV2:*IAR3*- and pTRV2:*GUS*-infiltrated plants. Microbial growth was 40% lower in pTRV2:*IAR31*- as compared to pTRV2:*GUS*-infiltrated plants (Fig. 5B). This result shows a positive correlation between larger necrotic lesions and a restriction of fungal spread. Display of the defense response was confirmed by quantifying defense markers: *HIN1*, at the transcript level and the pathogenesis related protein chitinase at the protein level. *HIN1* transcripts levels were 2-fold higher in pTRV2:*IAR31*- as compared with pTRV2:*GUS*-infiltrated plants at 2 dpi. In addition, chitinase protein levels increased 2.7-fold. These results suggest that despite the larger necrotic lesions observed, HR was not compromised in pTRV2:*IAR31*-infiltrated plants (Fig. 5C).

In order to obtain an additional insight, the expression level of two genes associated with the salicylic acid (SA) pathway, encoding phenylalanine ammonia lyase (PAL) and the pathogenesis-related protein 1a (PR1a) [28], were analyzed. None of them showed significant differences between the pTRV2:*IAR31*- and pTRV2:*GUS*-infiltrated plants (Fig. 5D).

3.5. *IAR3 expression is up-regulated in* C. fulvum*-inoculated tomato plants*

In order to further characterize IAR3 function, we used tomato cultivars MM-Cf0 and its near isogenic line MM-Cf4, in which the resistance gene *Cf-4* has been introgressed. MM-Cf0 and MM-Cf4 develop compatible and incompatible interactions respectively, upon inoculation with a *C. fulvum* strain carrying the avirulence gene *Avr4* [29]. Analysis of *IAR31* expression in this plant-pathogen system showed that *IAR31* transcript levels increased about 2- and 3-fold in MM-Cf0 and MM-Cf4 respectively, at 10 dpi with the fungus (Fig. S5).

3.6. *IAR3 silencing in tomato plants causes an increase in basal defense against* C. fulvum

Ten-days old MM-Cf0 and MM-Cf4 seedlings were infiltrated with pTRV2:*IAR31* aiming the silencing of *IAR3* genes expression. These plants exhibited a similar stunted phenotype as observed in *N. benthamiana IAR3* knocked-down plants (Fig. S6; compare to Fig. 4). As controls, MM-Cf0 and MM-Cf4 plants were infiltrated with pTRV2:*GUS* but no changes in the phenotype were observed. At 3 weeks after infiltration, the pTRV2:*GUS*- and pTRV:*IAR3*-infiltrated MM-Cf0 and MM-Cf4 plants were inoculated with a transgenic *Avr4*-carrying strain of *C. fulvum*, which also expresses the pGPD:*GUS* transgene. This strain was used as a reporter of pathogen proliferation. Thirteen days after *C. fulvum* inoculation, leaflets from compound leaves were analyzed for the presence of mycelia growth by performing a GUS activity stain. Fully resistant MM-Cf4 plants infiltrated either with pTRV2:*GUS* or pTRV2:*IAR3* did not show any fungal colonization, while pTRV2:*GUS*-infiltrated MM-Cf0 plants showed a characteristic susceptible phenotype after *C. fulvum* inoculation. On the other hand, pTRV2:*IAR31*-infiltrated MM-Cf0 plants showed a much lower level (about 40% less) of pathogen proliferation as compared to the pTRV2:*GUS*-infiltrated MM-Cf0 plants (Fig. 6A). As a positive control, MM-Cf4 plants were infiltrated with pTRV2:*Cf-4*, aiming to silence the *Cf-4* gene required to confer resistance to the *Avr4*-expressing *C. fulvum* strain. Mycelial growth was detected when pTRV2:*Cf-4*-infiltrated MM-Cf4 plants were inoculated with *C. fulvum* (Fig. 6A), evidencing the loss of full resistance due to a successful silencing of *Cf-4*.

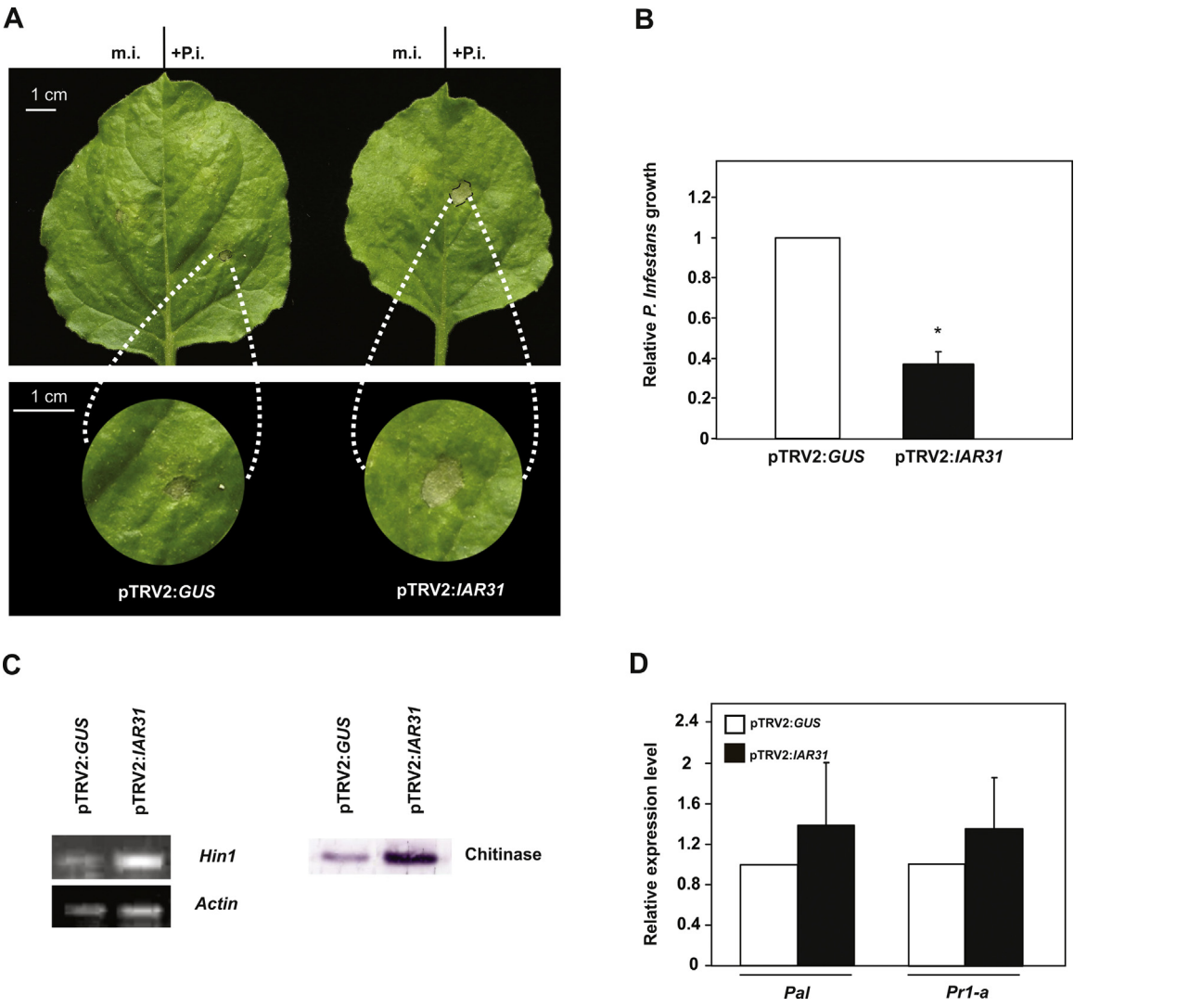

Fig. 5. Defense response of pTRV2:*IAR31*-infiltrated *N. benthamiana* plants inoculated with *P. infestans*. Three weeks after pTRV constructs inoculation plants were infiltrated with *P. infestans* on the right side of the leaves (+P.i.), or with a $MgCl_2$ solution on the left side. (A) Leaves were photographed two days after *P. infestans* inoculation. In the lower panel, a 2× magnification of the HR is shown. (B) Relative *P. infestans* growth in infected leafs of pTRV2:*GUS*- and pTRV2:*IAR31*- infiltrated *N. benthamiana* plants. Mycelium growth was measured in leaf disks incubated for 2 days and values were normalized to pTRV2:*GUS*-infiltrated plants. Data marked with an asterisk mean significant differences as assessed by Student's *t*-test at $P < 0.05$. Error bars represent the standard deviation from three biological replicates. (C) *HIN1* transcript (left panel) and chitinase protein expression (right panel) in pTRV2:*GUS*- and pTRV2:*IAR31*-infiltrated plants inoculated with *P. infestans* at 2 dpi. (D) Expression of salicylic acid-stimulated pathway marker genes PAL and PR1a in pTRV2:*GUS*- and pTRV2:*IAR31*-infiltrated plants at 2 dpi with *P. infestans*.

3.7. *IAR31 is downregulated in Cf-4/Avr4 tomato seedlings upon triggering of defense response*

To gain further insights into the role of IAR3 during the HR, we analyzed the expression level of *IAR3* in tomato seedlings that express a matching pair of resistance (*Cf-4*) and avirulence (*Avr4*) genes in the same plant [15]. The defense response that MM-Cf4 plants undergo when inoculated with a strain of *C. fulvum* expressing *Avr4* can be triggered without the participation of the pathogen. A systemic HR is mounted in the whole plant when the seedlings are exposed to a temperature and humidity shift (Fig. 6B). Using this model, we observed that the *IAR31* transcript levels decreased about 80%, as compared with the parental seedlings, at 8 h after the initiation of the Cf-4/Avr4-triggered defense response (Fig. 6C). This indicates that there is a downregulation of *IAR31* triggered by the interaction Cf-4/Avr4 in a pathogen-free system.

4. Discussion

So far, the IAA-AH gene family has been studied in Arabidopsis [4], *T. aestivum* [5], *B. rapa* [6] and *M. truncatula* [7]. In this work, we identified the IAA-AH family members of three Solanaceous species: tomato, potato and *N. benthamiana*. Phylogenic analysis supported an early divergence of the IAA-AH family, as evidenced by the occurrence of orthologs for most IAA-AH family members; *ILR1, ILL3, ILL6,* and *IAR3*, in Solanaceous species and in Arabidopsis. In addition, subsequent gene duplications occurred after divergence, as evidenced by the presence of two or more homologous genes for most IAA-AH family members.

A consistent *IAR3* up-regulation by biotic stress in potato tubers [11] and in this work, in tomato and *N. benthamiana* leaves (Figs. 2 S5), led us to initially hypothesize that IAR3 may have a role in the plant defense response. In agreement with that, transcription of the *Brassica rapa IAR31* homologue (*BrIAR3*) has been reported to be induced upon infection with the biotrophic pathogen *Plasmodi-*

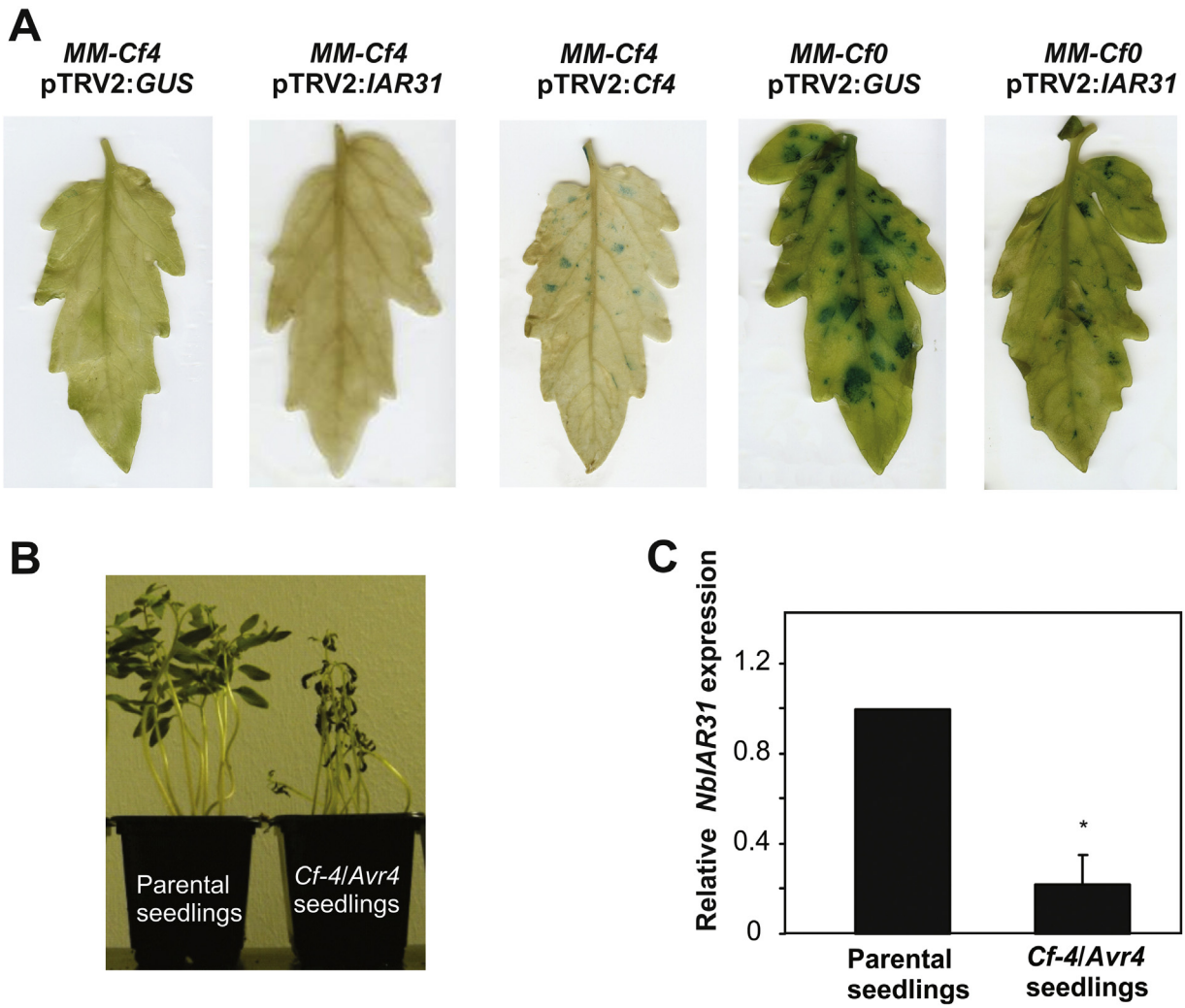

Fig. 6. Defense response of pTRV2:*IAR31*-infiltrated tomato to *C. fulvum* and IAR3 expression in *Cf-4/Avr4* tomato seedlings model. (A) Tomato plants MM-Cf4 and MM-Cf0, (that express the Cf-4 resistance gene or not, respectively) infiltrated either with pTRV:*GUS*, pTRV2:*Cf-4* or pTRV2:*IAR31* were inoculated with a strain of *C. fulvum* expressing *Avr4* (Cf-4 matching avirulence gene) and a GUS reporter construct at three weeks after infiltration. Colonization of the leaflets was studied with an X-gluc assay at 13 days after inoculation. Leaflets representative of three independent experiments are shown. (B) *Cf-4/Avr4* tomato seedlings grown at 33 °C and shifted to 20 °C to induce defense signaling (right). MM-Cf4 and transgenic *Avr4*-expressing seedlings were combined (parental lines) and treated similarly (left). (C) The expression level of *IAR31* in *Cf-4/Avr4* tomato seedlings and parental lines was determined at 8 h after the temperature shift. The expression level of the parental seedlings was assigned an arbitrary value of 1. Error bars represent the standard deviation from three biological replicates. The asterisk indicates significant difference as assessed by Student's *t*-test $P < 0.05$.

ophora brassicae [6]. However, the mechanism of such a regulation has not been explored yet. The up-regulation of IAA-AH genes has also been reported for the beneficial interactions between *M. truncatula* and symbiotic rhizobia or arbuscular mycorrhiza [7].

In order to gain insight into a possible role of IAR3 in defense response we performed *IAR3* silencing experiments in *N. benthamiana* and in tomato plants. VIGS-mediated *IAR3* knocked-down tomato and *N. benthamiana* plants showed consistently a stunted phenotype with reduced apical dominance, evidencing that auxin transport resulted altered. *IAR3*-silenced plants were also affected in auxin homeostasis; diminished levels of free IAA and oxo-IAA, the first precursor in the auxin inactivation pathway [1] were detected. In agreement with our results, it was recently reported that the knock-out of the expression of the IAA-amino synthetase *GH3.17-VAS2* generated plants with affected spatial distribution of auxins and increased levels of free auxin [30]. Interestingly, authors concluded that the local metabolism of auxins is able to regulate auxin homeostasis and transport in Arabidopsis hypocotyls [30].

Analysis of *IAR3* knocked-down tomato and *N. benthamiana* plants subjected to biotic stress showed consistently alterations in the defense responses. When *IAR3* knocked-down *N. benthamiana* plants were treated with an incompatible *P. infestans* race, altered necrotic lesion areas but higher expression levels of HR markers with a concomitant reduced pathogen spread was detected (Fig. 5). Similarly, *IAR3* knocked-down tomato plants susceptible to the pathogen *C. fulvum* presented increased basal defenses and reduced colonization when inoculated with this pathogen (Fig. 6). Previously, it was reported that plants with altered auxin homeostasis due to an enhanced expression of GH3 also exhibited resistance to biotic stress [31]. Modification in the auxin signaling was also reported to affect susceptibility to infection in Arabidopsis [32]. Defense response elicited by flg22 –the bacterial peptide derived from flagellin- includes a miRNA-mediated regulation of auxin receptor proteins that leads to the suppression of auxin signaling and restricts *P. syringae* growth [32].

According to Glazebrook [33], programmed cell death taking place in the host and the concomitant activation of SA-dependent defense responses are the main responsible of an effective defense against biotrophic pathogens. However, transcript levels of genes associated with the SA pathway were not significantly altered in

IAR3 knocked-down, more resistant plants (Fig. 5). In agreement with our result, it was reported that *P. syringae* manipulates auxin physiology via a SA-independent mechanism to promote pathogenesis in Arabidopsis [34]. Thus, low levels of free IAA do not per definition induce SA-mediated defenses. It has been proposed that auxins might have a physiological effect on plant tissues and cells that may benefit the progression of disease, such as for example cell wall loosening [35]. Interestingly, it has been also suggested that IAA might act as a signaling molecule for bacteria, being involved in the survival of the pathogen to the defense exerted by the plant [36].

Consistently, knocking down *IAR3* expression led to decreases in the pathogen spread, controverting the initial hypothesis of a role for *IAR3* in the defense response. In order to clarify whether *IAR3* up-regulation could be part of the plant defense response to pathogens, we took advantage of the model referred to as "dying seedlings", which allows studying several aspects of the defense response triggered by the specific recognition of Avr4 by Cf-4 in a pathogen-free system [15]. By using this model, we observed that the Cf-4/Avr4-triggered defense response did not include an increase in the amount of *IAR31* transcripts, but on the contrary, *IAR31* transcript levels had significantly decreased at 8 h after the initiation of the systemic defense response (Fig. 6). At this time point, the plants show massive expression of defense- related genes, indicating that the defense response is fully activated [15,37].

The alteration of auxin metabolism in the defense response should not be taken isolated from other responses in the plant that involve other plant hormones. For instance, a role for ethylene in plant defense has been found in the recent years [38–40]. As ethylene biosynthesis is transcriptionally up-regulated by auxin [41], when IAR3 is up-regulated, an increase of free auxin is expected and as a result, an increase in ethylene biosynthesis. It is also known that the ethylene-induced pathway has a negative effect on SA-dependent defenses [42]. Thus, an increase in IAR3 would not only directly favor infection spread as a result of higher levels of free auxin but also by promoting ethylene biosynthesis that in turn downregulates the SA-defense pathway. Supporting the participation of other plant hormones in the regulation of IAR3 expression, the scrutiny of the promoter region of *SlIAR31* identified responsive elements for absicic acid, ethylene, salicylic acid, drought, anaerobic stress, heat stress, fungal elicitor and light (Table S3).

On the other hand, it has been recently reported in Arabidopsis that IAR3 is a target of miR167 –that also targets different components of the auxin signaling pathway [43]. In addition, miR167 is known to be upregulated during incompatible infections [44]. Hence, downregulation of IAR3 might be also the result of miR167 activity as part of a more general response to downregulate auxin signaling pathway. Future work is intended to unravel regulatory pathways involved in IAR3 regulation.

Contrasting the results obtained for IAR3 regulation upon the onset of HR in the presence and in the absence of the pathogen, it could be suggested that the pathogen might target *IAR3* expression affecting IAA homeostasis in the host. The ability of bacterial and fungal pathogens to interfere with the auxin homeostasis has already been described for different pathosystems [45–47]. Nowadays, there is growing evidence that plant pathogens are able to modify IAA host homeostasis upon colonization and thereby manipulate host developmental processes in their own benefit [48]. To promote disease development, the necrotrophic fungus *B. cinerea* and the hemibiotroph *P. syringae* are able to hijack the metabolism of auxins of the host, causing to the accumulation of the IAA-conjugate IAA-Asp in Arabidopsis [10]. The compatible interaction between *M. truncatula* and the necrotrophic fungus *Macrophomina phaseolina* has been attributed to active down-regulation of *IAR34* expression [49].

Altogether, our results suggest that the increase in *IAR3* transcript levels that takes place upon pathogen challenge would not be part of the defense response to biotrophs and hemibiotrophs in Solanaceae. On the contrary, *IAR31* up-regulation could be the result of a manipulation of the host IAA homeostasis by the pathogens. Such manipulation would lead to changes in the levels of IAA metabolism compounds, such as increases in free IAA content, thereby favoring the spread of the infection.

Acknowledgements

S.D. is a postdoctoral fellow of Consejo Nacional de Investigaciones Científicas y Técnicas (CONICET). C.A.C. and D.F.F. are CONICET researchers. This research was funded by Agencia Nacional de Promoción Científica y Técnica, CONICET and Universidad Nacional de Mar del Plata. We thank Claudia V. Tonón for her technical assistance.

Appendix A. Supplementary data

Supplementary data associated with this article can be found, in the online version, at http://dx.doi.org/10.1016/j.plantsci.2016.09.008.

References

[1] A.W. Woorward, B. Bartel, Auxin: regulation, action, and interaction, Ann. Bot. 95 (2005) 707–735.
[2] J. Normanly, Approaching cellular and molecular resolution of auxin biosynthesis and metabolism, Cold Spring Harb. Perspect. Biol. 2 (2010) a001594.
[3] P.E. Staswick, B. Serban, M. Rowe, I. Tiryaki, M.T. Maldonado, M.C. Maldonado, W. Suza, Characterization of an Arabidopsis enzyme family that conjugates amino acids to indole-3-acetic acid, Plant Cell 17 (2005) 616–627.
[4] S. LeClere, R. Tellez, R.A. Rampey, S.P. Matsuda, B. Bartel, Characterization of a family of IAA-amino acid conjugate hydrolases from Arabidopsis, J. Biol. Chem. 277 (2002) 20446–20452.
[5] J.J. Campanella, A.F. Olajide, V. Magnus, J. Ludwig-Muller, A novel auxin conjugate hydrolase from wheat with substrate specificity for longer side-chain auxin amide conjugates, Plant Physiol. 135 (2004) 2230–2240.
[6] A. Schuller, J. Ludwig-Muller, A family of auxin conjugate hydrolases from Brassica rapa: characterization and expression during clubroot disease, New Phytol. 171 (2006) 145–157.
[7] J.J. Campanella, S.M. Smith, D. Leibu, S. Wexler, J. Ludwig-Müller, The auxin conjugate hydrolase family of *Medicago truncatula* and their expression during the interaction with two symbionts, J. Plant Growth Regul. 27 (2008) 26–38.
[8] T. Yamada, The role of auxin in plant-disease development, Ann. Rev. Phytopathol. 31 (1993) 253–273.
[9] S. Spaepen, J. Vanderleyden, R. Remans, Indole-3-acetic acid in microbial and microorganism-plant signaling, FEMS Microbiol. Rev. 31 (2007) 425–448.
[10] R. Gonzalez-Lamothe, M. El Oirdi, N. Brisson, K. Bouarab, The conjugated auxin indole-3-acetic acid-aspartic acid promotes plant disease development, Plant Cell 24 (2012) 762–777.
[11] S. D'Ippólito, M.L. Martín, M.F. Salcedo, H.M. Atencio, C.A. Casalongué, A.V. Godoy, D.F. Fiol, Transcriptome profiling of *Fusarium solani* f. sp. *eumartii* –infected potato tubers provides evidence of an inducible defense response, Physiol. Mol. Plant Pathol. 75 (2010) 3–12.
[12] C.M. Thomas, D.A. Jones, M. Parniske, K. Harrison, P.J. Balint-Kurti, K. Hatzixanthis, J.D. Jones, Characterization of the tomato *Cf-4* gene for resistance to *Cladosporium fulvum* identifies sequences that determine recognitional specificity in Cf-4 and Cf-9, Plant Cell 9 (1997) 2209–2224.
[13] X. Cai, F.L. Takken, M.H. Joosten, P.J. De Wit, Specific recognition of AVR4 and AVR9 results in distinct patterns of hypersensitive cell death in tomato, but similar patterns of defence-related gene expression, Mol. Plant Pathol. 2 (2001) 77–86.
[14] I.J. Stulemeijer, J.W. Stratmann, M.H. Joosten, Tomato mitogen-activated protein kinases LeMPK1, LeMPK2, and LeMPK3 are activated during the Cf-4/Avr4-induced hypersensitive response and have distinct phosphorylation specificities, Plant Physiol. 144 (2007) 1481–1494.
[15] C.F. de Jong, F.L. Takken, X. Cai, P.J. de Wit, M.H. Joosten, Attenuation of Cf-mediated defense responses at elevated temperatures correlates with a decrease in elicitor-binding sites, Mol. Plant Microbe Interact. 15 (2002) 1040–1049.
[16] A.B. Andreu, D.O. Caldiz, G.A. Forbes, Phenotypic expression of resistance to *Phytophthora infestans* in processing potatoes in Argentina, Am. J. Potato Res. 87 (2010) 177–187.

[17] P.J.G.M. De Wit, A light and scanning-electron microscopic study of infection of tomato plants by virulent and avirulent races of *Cladosporium fulvu*m, Neth. J. Plant Pathol. 83 (1977) 109–122.
[18] F.L. Takken, R. Luderer, S.H. Gabriels, N. Westerink, R. Lu, P.J. de Wit, M.H. Joosten, A functional cloning strategy based on a binary PVX-expression vector, to isolate HR-inducing cDNAs of plant pathogens, Plant J. 24 (2000) 275–283.
[19] C. Wu, L. Jia, F. Goggin, The reliability of virus-induced gene silencing experiments using tobacco rattle virus in tomato is influenced by the size of the vector control, Mol. Plant Pathol. 12 (2011) 299–305.
[20] Y. Liu, M. Schiff, S.P. Dinesh-Kumar, Virus-induced gene silencing in tomato, Plant J. 31 (2002) 777–786.
[21] S.H. Gabriels, J.H. Vossen, S.K. Ekengren, G. van Ooijen, A.M. Abd-El-Haliem, G.C. van den Berg, D.Y. Rainey, G.B. Martin, F.L. Takken, P.J. de Wit, M.H. Joosten, An NB-LRR protein required for HR signalling mediated by both extra- and intracellular resistance proteins, Plant J. 50 (2007) 14–28.
[22] M.H. Kumagai, J. Donson, G. della-Cioppa, D. Harvey, K. Hanley, L.K. Grill, Cytoplasmic inhibition of carotenoid biosynthesis with virus-derived RNA, Proc. Natl. Acad. Sci. U. S. A. 92 (1995) 1679–1683.
[23] M.W. Pfaffl, A new mathematical model for relative quantification in real-time RT-PCR, Nucleic Acids Res. 29 (2001) e45.
[24] S. Rozen, H. Skaletsky, Primer3 on the WWW for general users and for biologist programmers, Methods Mol. Biol. 132 (2000) 365–386.
[25] P.I. Dobrev, R. Vankova, Quantification of abscisic acid cytokinin, and auxin content in salt-stressed plant tissues, Methods Mol. Biol. 913 (2012) 251–261.
[26] P.I. Dobrev, M. Kaminek, Fast and efficient separation of cytokinins from auxin and abscisic acid and their purification using mixed-mode solid-phase extraction, J. Chromatogr. A 950 (2002) 21–29.
[27] Y. Takahashi, T. Berberich, K. Yamashita, Y. Uehara, A. Miyazaki, T. Kusano, Identification of tobacco HIN1 and two closely related genes as spermine-responsive genes and their differential expression during the Tobacco mosaic virus −induced hypersensitive response and during leaf- and flower-senescence, Plant Mol. Biol. 54 (2004) 613–622.
[28] D.S. Kim, B.K. Hwang, An important role of the pepper phenylalanine ammonia-lyase gene (PAL1) in salicylic acid-dependent signalling of the defence response to microbial pathogens, J. Exp. Bot. 65 (2014) 2295–2306.
[29] M. Joosten, P. de Wit, The tomato-*Cladosporium fulvum* interaction: a versatile experimental system to study plant-pathogen interactions, Ann. Rev. Phytopathol. 37 (1999) 335–367.
[30] Z. Zheng, Y. Guo, O. Novak, W. Chen, K. Ljung, J.P. Noel, J. Chory, Local auxin metabolism regulates environment-induced hypocotyl elongation, Nat. Plants 2 (2016) 16025.
[31] J.E. Park, J.Y. Park, Y.S. Kim, P.E. Staswick, J. Jeon, J. Yun, S.Y. Kim, J. Kim, Y.H. Lee, C.M. Park, GH3-mediated auxin homeostasis links growth regulation with stress adaptation response in Arabidopsis, J. Biol. Chem. 282 (2007) 10036–10046.
[32] L. Navarro, P. Dunoyer, F. Jay, B. Arnold, N. Dharmasiri, M. Estelle, O. Voinnet, J.D.G. Jones, A plant miRNA contributes to antibacterial resistance by repressing auxin signaling, Science 312 (2006) 436–439.
[33] J. Glazebrook, Contrasting mechanisms of defense against biotrophic and necrotrophic pathogens, Ann. Rev. Phytopathol. 43 (2005) 205–227.
[34] A.M. Mutka, S. Fawley, T. Tsao, B.N. Kunkel, Auxin promotes susceptibility to Pseudomonas syringae via a mechanism independent of suppression of salicylic acid-mediated defenses, Plant J. 74 (2013) 746–754.
[35] K. Kazan, J.M. Manners, Linking development to defense: auxin in plant-pathogen interactions, Trends Plant Sci. 14 (2009) 373–382.
[36] S. Spaepen, J. Vanderleyden, Auxin and plant-microbe interactions, Cold Spring Harb. Perspect. Biol. 3 (2011) a001438.
[37] D.W. Etalo, I.J. Stulemeijer, H.P. van Esse, R.C. de Vos, H.J. Bouwmeester, M.H. Joosten, System-wide hypersensitive response-associated transcriptome and metabolome reprogramming in tomato, Plant Physiol. 162 (2013) 1599–1617.
[38] B. Adie, J.M. Chico, I. Rubio-Somoza, R. Solano, Modulation of plant defenses by ethylene, J. Plant Growth Regul. 26 (2007) 160–177.
[39] O. Bouchez, C. Huard, S. Lorrain, D. Roby, C. Balagué, Ethylene is one of the key elements for cell death and defense response control in the arabidopsis lesion mimic mutant vad1, Plant Physiol. 145 (2007) 465–477.
[40] L.A.J. Mur, A.J. Lloyd, S.M. Cristescu, F.J.M. Harren, M.A. Hall, A.R. Smith, Biphasic ethylene production during the hypersensitive response in Arabidopsis: a window into defense priming mechanisms? Plant Signal, Behav 4 (2009) 610–613.
[41] L. Robles, A. Stepanova, J. Alonso, Molecular mechanisms of ethylene–auxin interaction, Mol. Plant 6 (2013) 1734–1737.
[42] O. Lorenzo, R. Solano, Molecular players regulating the jasmonate signalling network, Curr. Opin. Plant Biol. 8 (2005) 532–540.
[43] N. Kinoshita, H. Wang, H. Kasahara, J. Liu, C. Macpherson, Y. Machida, Y. Kamiya, M.A. Hannah, N.H. Chua, IAA-Ala Resistant3 an evolutionarily conserved target of miR167, mediates Arabidopsis root architecture changes during high osmotic stress, Plant Cell 24 (2012) 3590–3602.
[44] W. Zhang, S. Gao, X. Zhou, P. Chellappan, Z. Chen, X. Zhou, X. Zhang, N. Fromuth, G. Coutino, M. Coffey, H. Jin, Bacteria-responsive microRNAs regulate plant innate immunity by modulating plant hormone networks, Plant Mol. Biol. 75 (2011) 93–105.
[45] F. Llorente, P. Muskett, A. Sanchez-Vallet, G. Lopez, B. Ramos, C. Sanchez-Rodriguez, L. Jorda, J. Parker, A. Molina, Repression of the auxin response pathway increases Arabidopsis susceptibility to necrotrophic fungi, Mol. Plant 1 (2008) 496–509.
[46] R. Thilmony, W. Underwood, S.Y. He, Genome-wide transcriptional analysis of the *Arabidopsis thaliana* interaction with the plant pathogen *Pseudomonas syringae* pv. tomato DC3000 and the human pathogen *Escherichia coli* O157:H7, Plant J. 46 (2006) 34–53.
[47] Z. Chen, J.L. Agnew, J.D. Cohen, P. He, L. Shan, J. Sheen, B.N. Kunkel, Pseudomonas syringae type III effector AvrRpt2 alters Arabidopsis thaliana auxin physiology, Proc. Natl. Acad. Sci. U. S. A. 104 (2007) 20131–20136.
[48] K. Kazan, R. Lyons, Intervention of phytohormone pathways by pathogen effectors, Plant Cell 26 (2014) 2285–2309.
[49] K.M. Mah, S.R. Uppalapati, Y. Tang, S. Allen, B. Shuai, Gene expression profiling of Macrophomina phaseolina infected Medicago truncatula roots reveals a role for auxin in plant tolerance against the charcoal rot pathogen, Physiol. Mol. Plant Pathol. 79 (2012) 21–30.
[50] K. Tamura, D. Peterson, N. Peterson, G. Stecher, M. Nei, S. Kumar, MEGA5: molecular evolutionary genetics analysis using maximum likelihood, evolutionary distance, and maximum parsimony methods, Mol. Biol. Evol. 28 (2011) 2731–2739.